PORT SAID ENGINEERING RESEARCH JOURNAL

Faculty of Engineering - Port Said University
Volume 27 No. 4 pp: 90:101

Non-equal Channel Multi Angular Extrusion (NECMAE) – Part 2: The Role of Friction and Heat Generation due to Plastic Deformation

Noha Naeim [1,], Mohamed S. El-Asfoury [2]*

[1] *Department of Production Engineering and Mechanical Design, Port Said University, Port said, Egypt., email: noha.fouaad@eng.psu.edu.eg*

[2] *Department of Production Engineering and Mechanical Design, Port Said University, Port said, Egypt., email: mohamed.saad@eng.psu.edu.eg*

**Corresponding author,* *DOI: 10.21608/PSERJ.2023.237698.1261,*

Received 19-9-2023
Revised 4-10-2023
Accepted 4-10-2023

© 2023 by Author(s) and PSERJ.

This is an open access article licensed under the terms of the Creative Commons Attribution International License (CC BY 4.0).
http://creativecommons.org/licenses/by/4.0/

ABSTRACT

Among the procedures developed for structure grain refinement, equal channel angular extrusion techniques experience great popularity, owing to its their proficiency in producing significant grain refinement in fully dense bulk-scale materials. It is essential to compromise between the design of the die and the processing parameters to estimate a homogeneous deformation, optimize the strain distribution, and load requirement. In this regard, numerical modeling has been done to comprehend the impact of temperature and friction on the newly developed plastic deformation technique known as "nonequal channel multi-angular extrusion" (NECMAE), which experienced a cross-sectional area reduction on the subsequent channel. Three friction coefficients were examined and combined with heat generation analysis to evaluate the plastic strain homogeneity. The preliminary results obtained show that 30% reduction case with μ=0.1 has the most uniform strain distribution across the workpiece and improves strain homogeneity significantly by 6 times greater than the frictionless case. In general, the optimum strain distribution could be achieved by using the right combination of area reduction and frictional conditions. The analysis implies that plastic strain, temperature, and required load are significantly affected by localized plastic deformation zones and the incrementation of heat generated. The Current study opens the opportunity to satisfy the workpiece hardening level due to different localizations of plastic deformation of the proposed die design.

Keywords: Severe plastic deformation (SPD) , Finite element modeling (FEM) , Equal channel angular extrusion (ECAE), Friction coefficient.

1. INTRODUCTION

A simple shear was transformed into a potentially effective industrial technique after the invention of equal-channel angular extrusion (ECAE), which allowed for the excessive distortion of large billets. ECAE is the most fascinating method for the alteration of microstructure in the production of ultra-fine-grained materials (UFG) and was developed by Segal.[1] The process has made notable advancements in the following areas: grain refining to the nanoscale; refining of second phases and particles; healing of voids, pores, and other volume defects; improved diffusivity; texture management; geometric control of structural elements; aggregation and bonding of particulate matter; phase transformation; and improved superplasticity [2-4]. The procedure involved pressing the specimen into a die with two channels. This procedure exerts a lot of significant plastic strains on the specimen while keeping the cross-section proportions the same [5-8].

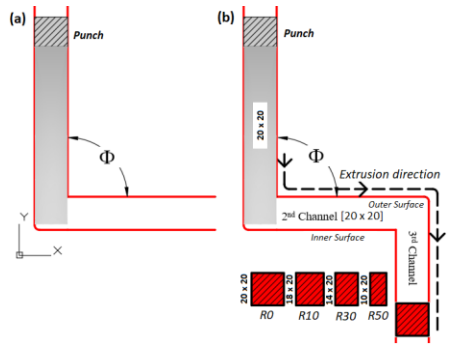

Figure 1: Conventional ECAE process (a), (b) Proposed NECAE with identified reduction dimensions.

Figure 1a shows a schematic drawing of an ECAE die of two channels with φ angle intersecting. Initially, the main goal of ECAE was to facilitate material processing by using a concentrated and consistent single shear force. However, the results illustrate that actual stress-strain states might deviate from the ideal deformation model and be more difficult [9, 10]. This was owing to a poor understanding of the most significant variables, such as friction of contact, channel geometry, and design of tool, in addition l to, the significant impact on back pressure and material properties[8]. At various structural levels with very high strains, continuous steady flow is replaced by localized discontinuous flow inside shear bands [11, 12]. The friction in the channels varies in many ways due to variations in processing conditions, allowing lubricated billets to be positioned immediately in the entry channel. Nevertheless, following the extrusion process, there is a possibility of the lubricating layer being disrupted, leading to localized shear on exposed, clean surfaces that can trigger the tool's response. The limiting condition of zero friction should be taken into account while evaluating this effect. Iwahashi [13] initially calculated analytically the mean equivalent strain (_N) generated by the workpiece throughout the ECAP process, as shown in Eq. (1):

$$\varepsilon_N = \frac{N}{\sqrt{3}}\left[2\cot\left(\frac{\Phi}{2}+\frac{\Psi}{2}\right)+\Psi.cosec\left(\frac{\Phi}{2}+\frac{\Psi}{2}\right)\right] \qquad (1)$$

where (N) denotes the number of pathways, (φ) denotes the die angle, and (φ) denotes the corner angle. The level of grain refinement attained by the ECAE process is significantly and directly impacted by the degree of plastic deformation and its homogeneity[14, 15]. Many approaches used slip line theory to calculate the cumulative strain and corresponding strain on the workpiece over a single pass[16]. Uniform friction, sharp edges, rounded corners, and various friction conditions between the input and exit channels were involved. In contrast, the aforementioned inquiry is a glorified case that does not consider the impact of friction, the inner corner, or the absence of filling in the outer corner. Nor does it have some proof of the behaviour of the front or end parts of the workpiece showing inhomogeneity.

Segal et al. [1] determined the shear that occurs if the misshaping region is distributed around the corner angle due to frictional impacts. This examination has shown that, under these circumstances, distortion is more unpredictable. As a consequence, it was discovered that many rounds of multi-pass ECAE processing, where the inner and outer surfaces are interchangeable, are required to achieve a higher level of uniformity. However, the impact of strain hardening is not well evaluated, particularly in the context of friction and multi-channel geometry. To predict the plastic behaviour during ECAE, the finite element modeling (FEM) is most often used in this manner. Shu et al. [17] researched the effects of die corners and multi-pass pressing on magnesium alloy. The author demonstrated that grain size can be refined and adopted after four passes with comparatively good mechanical properties. Wang et al.[18] created a redesigned die to reduce the potential for cracking and fracturing during ECAE. The billet was successfully extruded for 20 passes, compared to 13 passes in the conventional die. The enhancement is related to the reduction in tensile and highly compressive stress — the same concept as using back pressure. It has been demonstrated that, as theoretically expected for a perfect rigid-plastic material, back pressure causes the mode of deformation to change from gapped compression to simple shear [19]. Additionally, due to the homogeneous distribution of strain and stress, low-ductile materials may be extruded without failing. Evidently, ECAE leads to grain refinement which becomes more pronounced with increasing back pressure[20]. Back pressure increases the billet's friction against the channel walls, most noticeably at the bottom wall. Bowen et al. [21] showed that both friction and back pressure influence the flow behaviour in Equal Channel Angular Extrusion (ECAE), which are two interdependent factors. As an outcome, it is difficult to separate the effects of each component. Nevertheless, the resulting microstructure and texture are enhanced, the role of hydrostatic pressure in the process is undoubtedly significant.

The impact of friction was examined by Kuncicka et al. [22]. The investigation concentrated on the formation of a dead zone as friction increased. Despite the decrease in dead zone angle, inhomogeneity prevailed. Parshikov et al. [23] demonstrate that irregular shear strain distribution is a common feature of ECAE and that irregularity may be reduced using frictional conditions and die geometry. The ratio of the outer radius to the channel width had the greatest influence. The Friction coefficient and pressure speed have a significant influence on temperature rise during the process, according to a 3D modelling study by Shaban et al. [24]. Furthermore, Chung et al. [25] investigated that non-uniform deformation with extended strain contours was found because of the backward dragging force caused by friction at workpiece or die surfaces.

However, the strain per pass is restricted by a minimum die angle of 90°, which brings about a most

extreme compelling strain of 1.15 (Ψ=0), and few repeated extrusions are needed to accomplish high strains. It has been generally expected in the literature[26, 27] that the aggregate strain after a few extrusions can be acquired by essentially reproducing Eq. (1) by the number of extrusion cycles. Besides, few studies care about temperature's role in ECAE, which is important, especially in hard-to-work materials. It is worth mentioning that the strain hardening capability of UFG materials tends to diminish with increasing accumulative strain, which typically correlates to poor ductility at room temperature. In practice, the formability of age-hardenable alloys decreases when precipitates form during intense shear strain occurring during each ECAE pass[28]. Therefore, it is anticipated that the material will fracture or segment during the ECAE process at room temperature. These issues can be prevented or mitigated by raising the extrusion temperature and employing backpressure [29]. Furthermore, heat generation due to friction and deformation is not well understood. Hence, It is essential to take into account the friction and heat generation to simulate the real practical case. From all previous mentions, the combination between all parameters is continually missed; no trial results have been displayed to check this presumption. The improvement is usually restricted to modified die geometry, friction, or temperature individually. In this paper [30], FEM is used to present and analyze a novel non-equal channel multi-angular extrusion (NECMAE) technique. There are two stages to the procedure: the first stage is a standard ECAE procedure, the second stage uses various reduction ratios. The sample width has been lowered by 10%, 30%, and 50% relative to the initial width in three different degrees of reduction, as presented in Fig. 1b. To fully understand our modified design, in the current study, finite element analysis has been presented and investigated the impact of various friction coefficients and the role of temperature on the deformation performance. and to eliminate the need for experimental complexities. The new design offers a satisfactory uniform strain distribution in terms of friction and temperature. A Special focus is paid to the magnitude of the generated plastic strains as well as the homogeneity of plastic deformation over the width of the workpiece.

2. FINITE ELEMENT MODELLING

The commercial FE software ABAQUS/Explicit was used to construct a thermo-mechanical two-dimensional plane-strain FE of square cross-section pure aluminium with dimensions 20x20x160 mm3 using explicit dynamic analysis. An extensive explanation of the model, together with information on the workpiece, die, and mechanical parameters, were reported in [30, 31]. The workpiece was simulated using 4-node iso-parametric plane-strain elements (CPE4R), assuming a rigid plastic behaviour with strain hardening properties. A lagrangian formulation with continuous remeshing was used to reduce mesh distortion. The overall number of nodes ranges from 3380 to 4500 elements according to the mesh sensitivity analysis and the degree of distortion of the specimen. The workpiece was initially subjected to a temperature of 150°C, while the die temperature remained constant at 150°C throughout the analysis, serving as the processing temperature. The selection of temperature is determined by the precipitation hardening of the aluminum alloy, which is activated between 120 and 180 °C [32]. In addition, it will improve the workability of the materials, thereby preventing the formation of shear cracks caused by intense plastic deformation of the reduction.

Heat generation due to friction and plastic deformation was considered. The punch was also assumed to be rigid and was assigned a downward speed of 1 mm/s (similar to the experimental facility conducted by [33]), and the die was completely immobilized in its position throughout the process. The basic Coulomb friction model was utilized in the current investigation, which links friction stress to normal stress and friction coefficient. The friction coefficient (μ) was predicated on three different values namely 0, 0.1, and 0.2, consisted of other studies [34, 35]. The analysis was carried out to evaluate the influence of friction on the corner angle, deformation pattern, strain distribution, and required load during the four different NECMAE processes, each reducing their area by various percentages for the second channel. The four dies utilized in the study were labelled as R0, R10, R30, and R50, representing reductions in area of 0%, 10%, 30%, and 50%, respectively. The initial validation of the current model involved assessing its predicted equivalent plastic strain (PEEQ) values, which is a critical parameter in ECAE. These predicted values were compared to analytical predictions across a spectrum of corner angles, spanning from 0° to 90°. The maximum variation is around 5%, confirming the accuracy of the current models. The detailed validation was previously published in[30].

3. RESULTS AND DISCUSSION

3.1 Effect of friction coefficient on corner gap angle (α)

The study was executed on the ECAE at three different friction coefficients (0, 0.1, and 0.2, respectively). The resultant corner gap angle (α) acquired at the considered area reductions of 0%, 10%, 30%, and 50%. Figure 2 shows the impact of friction coefficient on corner gap angle (α) for various area reductions at the first intersection.

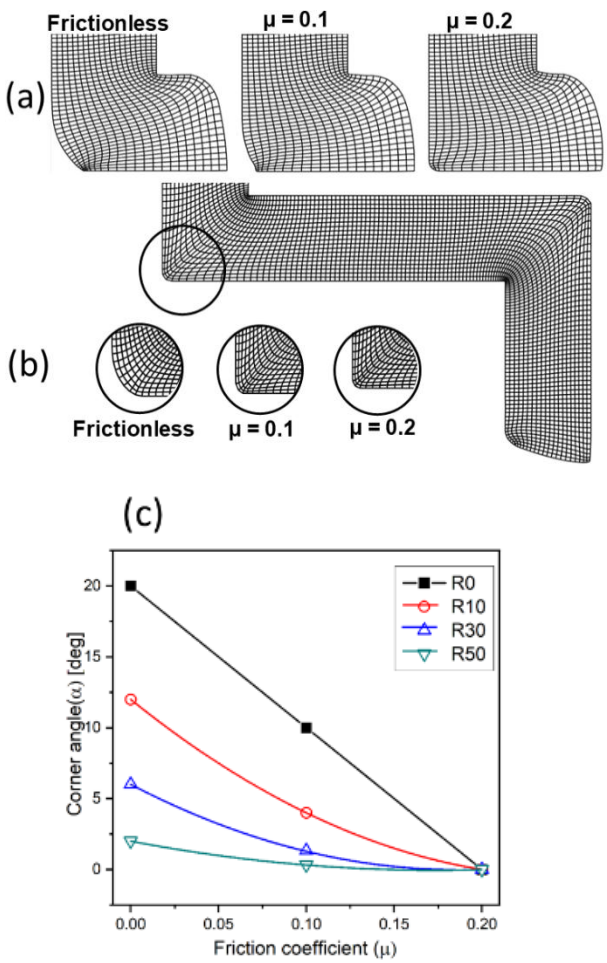

Figure 2: The impact of the friction coefficient on the corner gap angle (α) at the first intersection, (a) as material passes the first intersection, (b) after passing the second intersection for model R0, and (c) corner angle values for all models.

It can be noticed that the maximum corner angle was obtained at the minimum coefficient of friction with a 0% reduction of area. However, as the coefficient of friction and reduction in area increased, the corner angle decreased. The deformation zone decreased to its narrow size with friction increase and inhibition of sliding, as presented in Fig. 2a, with the corner almost absent for all models. Surprisingly, the second intersection angles were hardly noticeable (especially for μ values). Both back pressure from reductions and high accumulated friction on surfaces until the second intersection contributed to the same attitude towards various friction levels. This could be explained by higher heat generation brought on by friction, which increases temperatures and causes thermal softening. The minimum value of the corner angle occurred at a friction coefficient of 0.2 and a 50% reduction of area. The lower rate of corner gap angle reduction at the second intersection than at the first intersection, despite the strain hardening effects experienced in the latter, is considered to result from increased heat generation, which facilitates the extrusion process because of thermal softening. As will be explained, a second intersection with a somewhat higher corner angle is effective in releasing the plasticity of the inner side of the first stage, as proved by a mathematical model in a previous study.

3.2 Effect of friction coefficient on Equivalent Plastic Strain (PEEQ)

Figures 3 (a and b) illustrate the equivalent plastic strain distribution (PEEQ) for the second channel before the workpiece material enters the third stage. In addition, the third channel is opened after entering the third stage at various values for the friction and reduction areas.

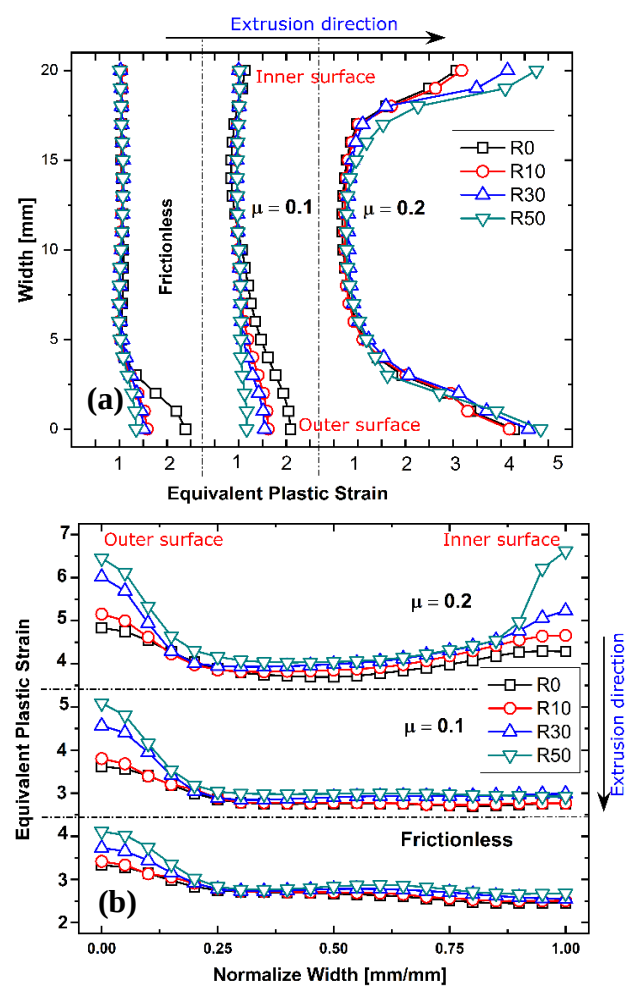

Figure 3: Equivalent plastic strain distribution (PEEQ) across (a) the second channel and full specimen passes at different friction values, (b) the third channel with respect for different reduction area.

Fig. 3a shows the impact of friction on equivalent plastic strain after the workpiece has crossed the second intersection. The strain distribution only exhibits a lack of

uniformity when there is no friction, or even when μ=0.1 and conventional multi-channel case (R0). The trend is essentially the same for μ = 0 and μ = 0.1. In contrast, higher PEEQ magnitudes occur at higher friction and the outer surface. Iwahashi's calculations show that the current die design's single pass strain is 1.15 [13]. Strains of frictionless and 0.1 cases differentiate only on 25 and 40% of the sample width, respectively, with the remaining width being near to analytical value (the strain variant between 0.99 and 1.07, which is a good agreement). It is significant to note that, as extrusion temperatures increase, the strain on the workpiece decreases. This may be due to the shear bands' sharpness being greatly decreased [36].

The conduct of μ=0.2 case was extrema, with normal values in the 50% width core but the highest PEEQ values in the outer surfaces (exceed 4.5). Area reduction was found to have a significant effect on the magnitude of plastic strain (PEEQ) close to the outer surface [the PEEQ distributions over the entire workpiece are shown in Fig.4]. This might be explained by the fact that the bottom side of the third channel shows greater evidence of the back pressure effects caused by area decrease than the upper side. The reduction area induced high friction on the outer surface, so non-equal friction led to the retraction of the corner gap and a greater spread into the first channel. In μ = 0.1 cases, area reduction resulted in a more gradual drop in PEEQ near the die outer surface; however, the effect of area reduction extended deeper into the workpiece compared to the frictionless case. This method is based on satisfying the impact of back pressure and avoiding the undesirable addition of friction value. This emphasises the importance of striking a balance between the back pressure produced by reduction of area and the coefficient of friction values.

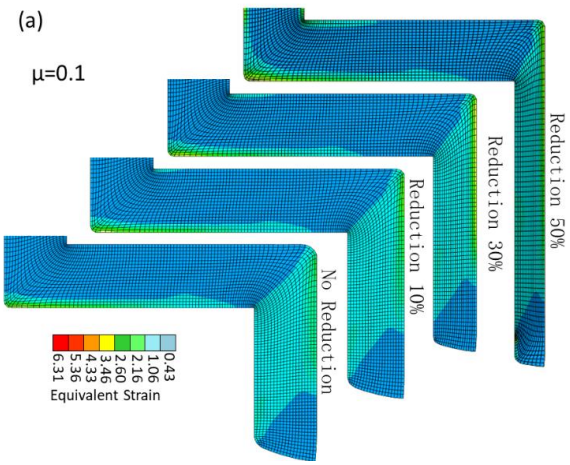

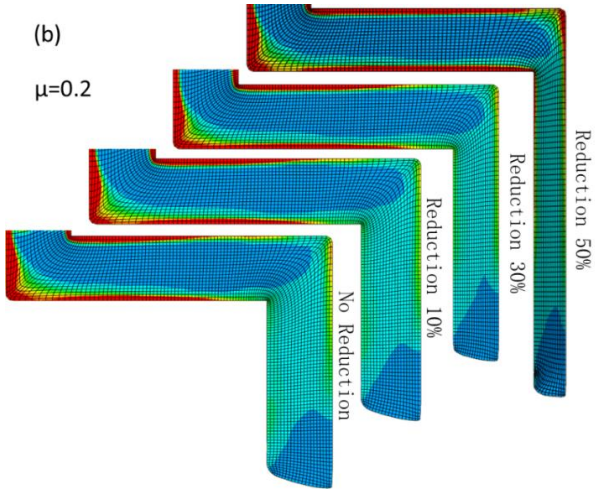

Figure 4: PEEQ distribution of materials with various reduction rations and friction coefficient of (a) 0.1, (b) 0.2.

As seen in Fig. 3, the magnitude of near-surface PEEQ is significantly greater than in other cases. However, area reduction had essentially little influence on PEEQ in most of the workpiece cross- sections, resulting in a more homogeneous PEEQ distribution than that attained in the interior zone. The considerable rise in plastic strain may be attributable to the severe plastic distortion occurring in the second intersection, and the increase in temperature caused by high friction and the decrease in the temperature value tempered the impact of friction in this case. This behaviour is consistent with the results of corner gap angles (Fig. 2), where a high friction coefficient cancels out the effect of extrusion at the second junction. However, the symmetric behavior of the μ = 0.2 model can be characterized surface deformation gradient or a sandwich structure. During plastic deformation combined with high friction, the material experiences varying levels of stress and strain, leading to changes in its microstructure and mechanical characteristics, and forming a layered structure. Due to this mismatch in properties between the faces and the core, stress concentrations can occur at these interfaces, frequently leading to delamination, which is a significant concern. Understanding this behavior is important for optimizing the processing conditions and designing materials with tailored properties.

Fig. 3b shows the impact of friction on the equivalent plastic strain distribution (PEEQ) of the third channel after entering the third stage for the normalized distance across the workpiece's final width for varied friction and reduction area values. For the first two friction levels (μ = 0 and μ= 0.1), the trend is approximately the same. In addition, at the outer surface and μ = 0.1, the maximum PEEQ is 5. For the third level of friction (μ = 0.2), the equivalent plastic strain at the outer surface is larger than the equivalent plastic strain at the inner surface for R0, R10, and R30. When R50 is obtained, the equivalent plastic strain (PEEQ) at the inner surface exceeds the

equivalent plastic strain at the outer surface. The strain values increased as a result of strain increment in the successive passes and plastic distortion as a result of area decrease. The same concept applies to strain distribution across the width of the workpiece.

3.3 Strain inhomogeneity

To quantify the amount of strain inhomogeneity throughout the width of the deformed specimen, a strain inhomogeneity index, C_{i}, was defined by Eq. (2) [37]:

$$C_{i,} = \left(Max\ \varepsilon_p - Min\ \varepsilon_p\right)/Avg.\varepsilon_p \qquad (2)$$

Where Max Ɛp and Min Ɛp and Avg. Ɛp represents the maximum, minimum, and average of the equivalent plastic strains along the billet width, respectively. Figure 5 shows the calculated strain inhomogeneity index Ci at different friction coefficients across the second and third channel, respectively.

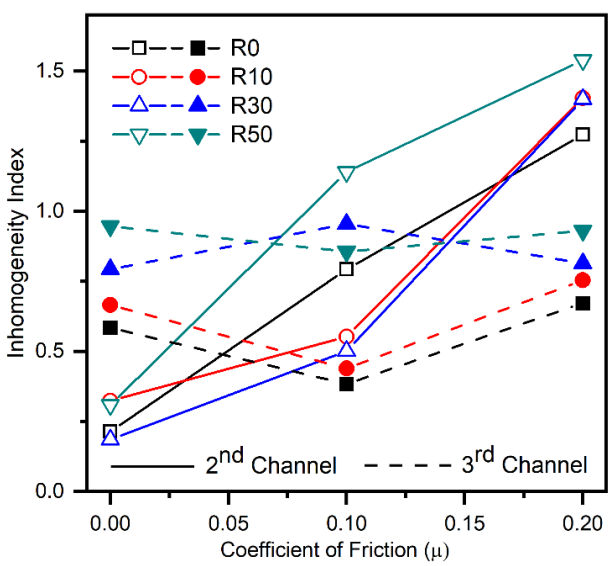

Figure5: Variation in inhomogeneity with respect for friction coefficients over the second and third channels.

As presented in Fig. 5, the frictionless cases had the most homogeneous strain throughout the second channel, with no observable improvement as reduction increased. However, increasing the friction value to 0.1 side by side by reduction up to the R30 model improves strain homogeneity significantly by 6 times greater than the frictionless case. The decrease in Ci at these friction coefficients is attributable to a greater increase in Min Ɛp when compared to Max Ɛp. These results agree with [37], and [38] investigations. However, the inhomogeneity index demonstrates limited variation across the third channel. The variance in PEEQ decreased when the workpiece underwent more intersections (passes). More relevant are the works performed by Wongsa et al. on Cu-Zr alloys with analysis parameters close to this study[39].

3.4 Effect of Friction on Temperature Distribution

Temperature has a significant influence on material deformation. In ECAE, the heat generated is proportional to the plastic deformation and due to the friction effect. According to these cautions, the friction coefficient must be considered a significant factor that generates heat. Model R50 was chosen for its high reduction ratio to show the temperature distribution at varied friction coefficients in the first and second stages. Figure 6 shows the temperature distribution across the workpiece at different friction coefficients after full passes.

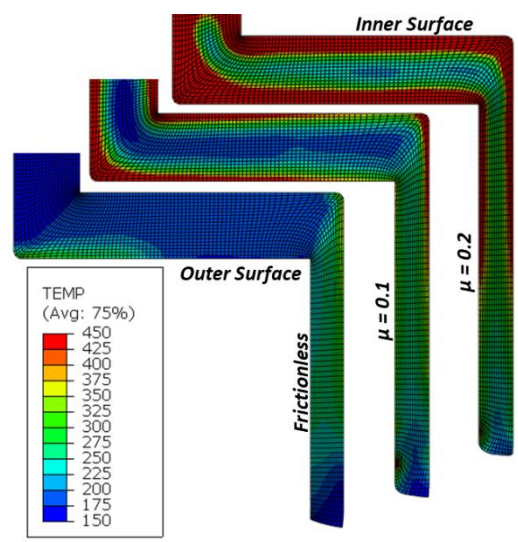

Figure 6: Temperature distribution over workpiece at different friction coefficients for model R50.

As seen, the temperature across the sample is not uniformly or equally distributed over the two stages. Also, the temperature increases with the increase in the coefficient of friction. The minimum temperature was 150°C for μ =0, while the maximum temperature was 450°C for μ =0.2.

Figure 7 (a, b) shows the effect of the frictional coefficient on temperature variation for the chosen model at varied friction coefficients at the inner and outer points in the first and second stages.

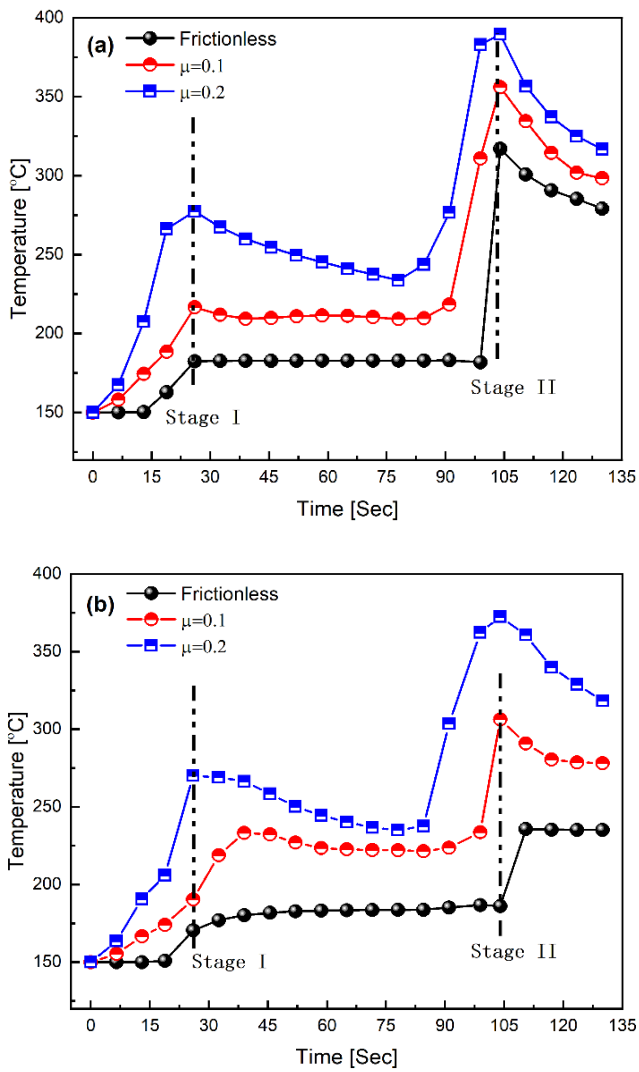

Figure 7: The effect of different friction coefficients on temperature variation for Model R50 at (a) the inner, and (b) the outer surfaces.

It is apparent that the temperature values for the first stage at the inner and outer points are the same, which is due to the same formation conditions. At the first stage and on both surfaces, temperature increases with friction, with nearly identical values (180, 220, and 280 °C for μ = 0, 0.1, and 0.2, respectively). The temperature rises with ram progress, reaching its peak value at the first and second intersections (approximately 15% and 70% of the stroke length, respectively). The temperature behaviour of both surfaces after the second intersection was the same as when friction increased, but the temperature sensation for the inner surface was higher even in the frictionless case. Temperature rises as a result of friction, and the sharp angle on the inner corner allows the temperature to be generated at the metal-metal interface. On the other side, in the outer corner, the temperature can be dissipated through the deformation of the outer surface. The temperature of the workpiece gradually reduces after the second intersection, owing to heat transfer from the workpiece to the die. As a result, the temperature variance between the two surfaces was reduces as friction increases. This behaviour was evident for all models but was more pronounced for R50 when compared to the other reductions [see Fig.8]. Practically, temperature control with friction influence could vary the grain refining concept [40]. Regulating the temperature of both friction and processing could influence the dynamic recovery and grain growth processes[41].

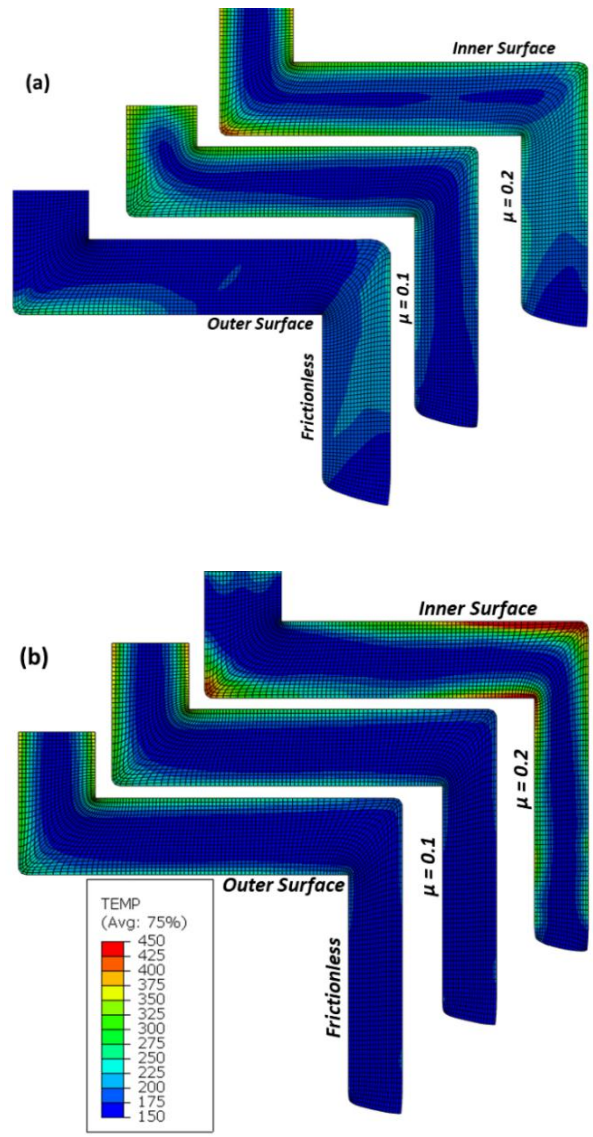

Figure 8: Temperature distribution over workpiece at different friction coefficients for (a) Model R10, and (b) Model R30.

3.5 Effect of Friction on Load-stroke

The force required by ECAE deformation is defined by the mechanical characteristics of the processed material, friction, and the geometry of the tool system and workpiece. According to previously published data, in the frictionless case and at the first stage, the force required to get the material through the first deformation stage (from channel one to channel two) is approximately 5.5–6 tons, while in the second stage, the force is approximately 13–13.5 tons for cases R0–R30 and 16.5 tons for case R50 [30].

Figure 9 shows the relationship between the extrusion force required and the punch travel for all models at μ=0.1 and 0.2. The initial deformation zone's resistance increases the load required to deform the workpiece.

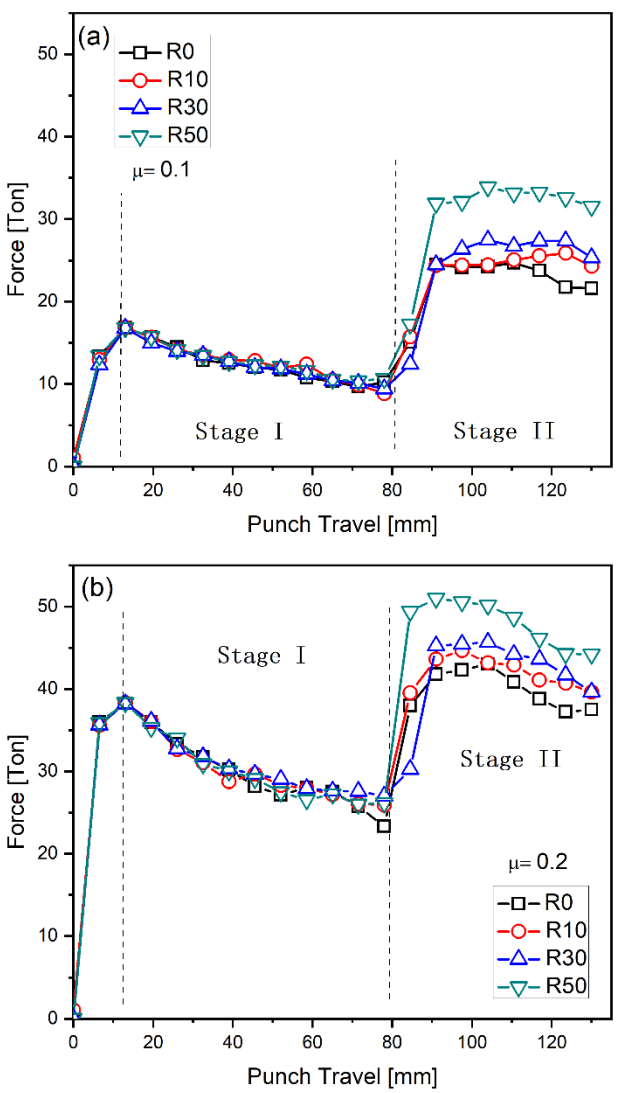

Figure 9: Punch displacement with extrusion force for all reduction models at (a) μ=0.1, and (b) μ=0.2.

Furthermore, when the workpiece material fills the deformation zone and begins to slide on the outer channel surface, the load reaches its peak. Shear plastic strains are caused by the relative motion of the inner and outer surfaces of the workpiece. When the workpiece's front end exits the deformation zone, steady-state shear deformation occurs, and the load reaches a steady-state value. As seen in Fig. 9, the first intersection has peaks of 19 and 40 tons for μ= 0.1 and 0.2, respectively. However, the required load for the second stage was different, as predicted, because the difference between different cases (R0–R50) is only apparent in the second stage, when an area decrease occurs. This is due to two main reasons: First, the workpiece material experiences a back pressure effect (resistance) when it passes through the second stage; second, the material experiences strain hardening effects after plastic deformation in the first stage. In all friction models, the 50% reduction model shows a smooth increase. The comparison indicates that the required force for all reduction ratios was almost identical, except for model R30. The comparison shows that the required force for all reduction ratios was in almost the same range except for model R30. As a result, a 50% reduction ratio has a significant influence on hardening material, even when the temperature is absent.

3.6 Effect of heat factor on Equivalent Plastic Strain (PEEQ)

According to the results of the deformation process, the workpiece subjected to plastic deformation localises in the deformation zones and intervenes as thermal softening overcomes strain hardening, which is often the precursor of the plasticity experience. The models were re-analyzed using mechanical principles, with no possibility of heat dissipation throughout the process (no inelastic heat factor). This analysis was performed for all frictionless reduction models to isolate the influence of heat generated by plastic deformation on PEEQ values and required load. Figure 10 (a and b) illustrates the effect of plastic distortion on PEEQ and temperature.

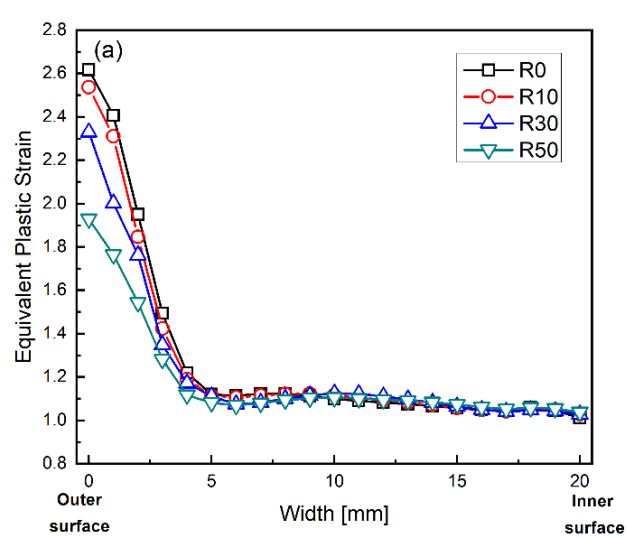

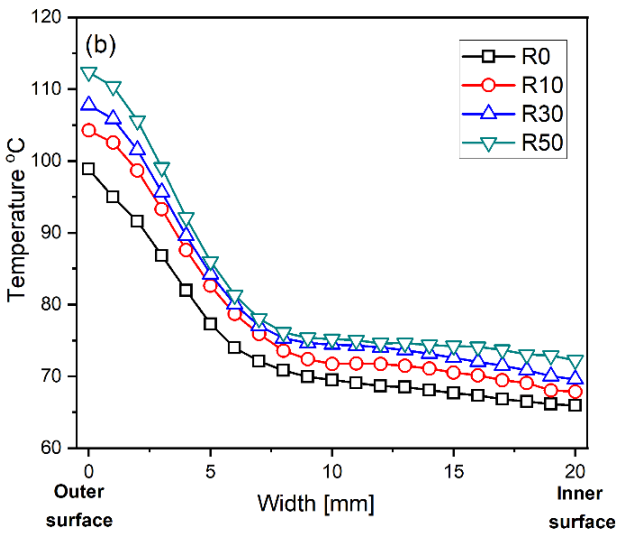

Figure 10: Effect of plastic distortion on (a) PEEQ (b) Temperature.

Figure 10a illustrates the impact of plastic distortion on PEEQ through different reduction models (over the second channel). The behaviour of equivalent plastic strain was similar to that seen in Figure 2, but the variance in values was very limited. This behaviour emphasises the significance of heat dissipated by plastic deformation, which is localised in shear zones. The PEEQ had a value of around 2.5 and was only applied to the exterior. This value was private for the non-reduction model in coupled analysis (see Fig. 2). An analysis at room temperature and heat factor authorization was performed to investigate the temperature influence on plastic deformation, as shown in Figure 10b. As seen, the temperature increased as the reduction ratio increased; in addition, the temperature impact was mostly high at the outer surface and progressively decreased until it reached the inner surface (the temperature difference was 5 to 0.2 °C). It can be concluded that temperature has a significant influence on plastic deformation due to area reduction. This behaviour is related to strain softening (strain hardening properties) and thermal softening from heat fraction. The investigation was expanded to study the extrusion force required at room temperature and at the initial temperature.

The analysis was expanded to investigate the extrusion load required. Figure 11(a, b) shows the loads required at different heat factors (HF=0, 0.9) and processing temperatures (27, 150˚C).

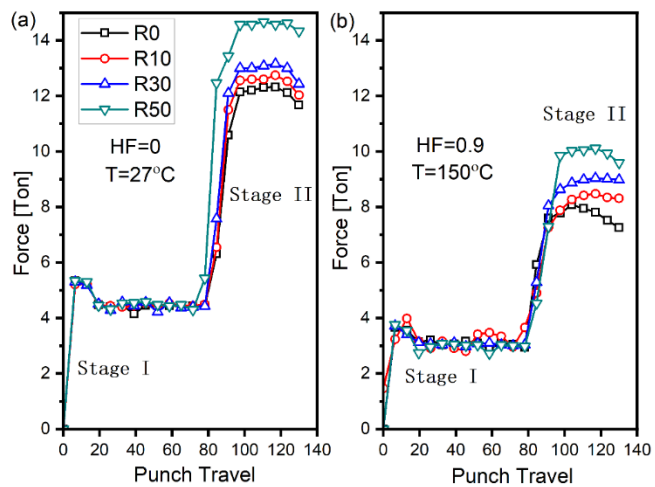

Figure 11: Comparison of extrusion force during different heat factors and processing temperatures, (a) HF=0, T=27˚C, and (b) HF=0.9, T=150˚C.

A higher heat factor would result in faster heat input and a higher temperature rise in the material as extruded, while a lower heat factor would result in a slower heat input and a lower temperature rise. As predicted, the force decreased as the temperature increased, as shown in Fig 11b. The load differential for the first stage was up to 1 ton and increased to 4 tons for the second stage. Heat generated by plastic deformation and friction has a significant influence on material softening. Furthermore, without the heat effect, separated layers of the workpiece may exist due to differing levels of plastic strain. A compromise between heating temperature and friction coefficient is essential to achieve homogeneity. Using die heating without considering friction will thus increase overall strain on the workpiece without achieving the required homogeneity. Considerable friction coefficients in the analysis have the opportunity to satisfy the workpiece hardening level due to different localizations of plastic deformation between workpiece surfaces. Precautions should be differentiated according to material properties; in superplastic metal, for example, aid with temperature is important; in soft metal, the opposite is required. More analysis is required to specify this critical situation. Finally, by comparing the current results to the previous investigations, we observed agreement in the increasing the coefficient results, and it was found that by of friction, the maximum ε_p rises [42]. In addition, the NECAP of a magnesium alloy has shown similar results in publications[43]. Moreover, the Dead Metal Zone is created on the outside of where the two channels intersect when the ratio of the output channel's width to the input channel's width is increased. Furthermore, the corner gap is created on the outer side of the intersection of the two channels when the width of the output channel to the input channel is increased, while the amount of applied strain is reduced on the bottom side of the deformed sample. With a reduction in output channel width, more pressing force is needed to complete the NECAP process.

4. CONCLUSION

The role of friction in the proposed MNECAE process depends on the plastic strain behaviour, deformation inhomogeneity, and required load, which were studied using FEM analysis on three reduction models on the third channel, namely (R10, R30, and R50), and three friction values (frictionless, 0.1, and 0.2). According to the obtained results, friction affects the plastic strain distribution, dissipated temperature, and load required on the workpiece under the MNECAE process. The corner angle decreases as friction increases for all reduction models, and similarly for R30 and R50 models. The best plastic strain homogeneity across the workpiece width belongs to the R30 model with a 0.1 friction value. The workpiece experienced strain hardening due to plastic distortion during the first stage. Therefore, the load needed to deform a strain hardening material in a MNECAE process was similar up to the first stage and increased incessantly with the increase in reduction area. The role of temperature across the workpiece because of friction or deformation and the related heat generated were discussed. The analysis implies that plastic strain, temperature, and required load are significantly affected by the localized plastic deformation zone and the increments of heat in this region. This study gave a useful indication of the MNECAE's capability and formability. Practically, according to the material properties, this study could manage the pre-processing parameters are to implement MNECAE fruitfully for the desired properties.

Acknowledgments

A preliminary analysis of the data reported in this work was presented in condensed form at the 7th International Conference on Computational Methods and Experiments in Materials, March 2015, in Valencia, Spain, and published in WIT- Press,

5. REFERENCES

[1] V. J. M. S. Segal and E. A, "Equal channel angular extrusion: from macromechanics to structure formation," Materials Science and Engineering: A, vol. 271, no. 1-2, pp. 322-333, 1999. doi: 10.1016/S0921-5093(99)00248-8.

[2] S. C. Wang, M. J. Starink, N. Gao, X. G. Qiao, C. Xu, and T. G. J. A. m. Langdon, "Texture evolution by shear on two planes during ECAP of a high-strength aluminum alloy," Acta Materialia, vol. 56, no. 15, pp. 3800-3809, 2008. doi: 10.1016/j.scriptamat.2008.09.036.

[3] G. J. Raab, R. Z. Valiev, T. C. Lowe, Y. T. J. M. S. Zhu, and E. A, "Continuous processing of ultrafine grained Al by ECAP–Conform," Materials Science and Engineering: A, vol. 382, no. 1-2, pp. 30-34, 2004. doi: 10.1016/j.msea.2004.04.021.

[4] E. Cerri, P. De Marco, and P. J. j. o. m. p. t. Leo, "FEM and metallurgical analysis of modified 6082 aluminium alloys processed by multipass ECAP: Influence of material properties and different process settings on induced plastic strain," journal of materials processing technology, vol. 209, no. 3, pp. 1550-1564, 2009. doi: 10.1016/j.jmatprotec.2008.04.013.

[5] M. Furukawa, Z. Horita, T. G. J. M. S. Langdon, and E. A, "Factors influencing the shearing patterns in equal-channel angular pressing," Materials Science and Engineering: A, vol. 332, no. 1-2, pp. 97-109, 2002. doi: 10.1016/S0921-5093(01)01716-6.

[6] M. S. El-Asfoury, M. N. Nasr, K. Nakamura, and A. J. J. o. E. M. Abdel-Moneim, "Structural and Thermoelectric Properties of Bi 85 Sb 15 Prepared by Non-equal Channel Angular Extrusion," Journal of Electronic Materials, vol. 47, pp. 242-250, 2018. doi: 10.1007/s11664-017-5755-7.

[7] R. Mohan, R. Venkatraman, and S. J. J. o. M. E. Raghuraman, "ANALYSIS ON DEFORMATION BEHAVIOR FOR PURE COPPER PROCESSED THROUGH EQUAL CHANNEL ANGULAR PRESSING DIE," Journal of Manufacturing Engineering, vol. 8, no. 2, pp. 114-116, 2013.

[8] S. Li, M. Bourke, I. Beyerlein, D. Alexander, B. J. M. S. Clausen, and E. A, "Finite element analysis of the plastic deformation zone and working load in equal channel angular extrusion," Materials Science and Engineering: A, vol. 382, no. 1-2, pp. 217-236, 2004. doi: 10.1016/j.msea.2004.04.067.

[9] W. Kim, J. Namgung, and J. J. S. m. Kim, "Analysis of strain uniformity during multi-pressing in equal channel angular extrusion," Scripta materialia, vol. 53, no. 3, pp. 293-298, 2005. doi: 10.1016/j.scriptamat.2005.04.014.

[10] N. Medeiros, J. Lins, L. Moreira, J. J. M. S. Gouvea, and E. A, "The role of the friction during the equal channel angular pressing of an IF-steel billet," Materials Science and Engineering: A, vol. 489, no. 1-2, pp. 363-372, 2008. doi: 10.1016/j.msea.2008.01.011.

[11] J.-H. Lee, I.-H. Son, Y.-T. Im, S. Chon, and J. K. J. J. o. m. p. t. Park, "Design guideline of multi-pass equal channel angular extrusion for uniform strain distribution," Journal of Materials Processing Technology, vol. 191, no. 1-3, pp. 39-43, 2007. doi: 10.1016/j.jmatprotec.2007.03.055.

[12] H. S. J. M. S. Kim and E. A, "Finite element analysis of deformation behaviour of metals during equal channel multi-angular pressing," Materials Science and Engineering: A, vol. 328, no. 1-2, pp. 317-323, 2002. doi: 10.1016/S0921-5093(01)01793-2.

[13] Y. Iwahashi, Z. Horita, M. Nemoto, J. Wang, and T. G. J. S. m. Langdon, "Principle of equal-channel angular pressing for the processing of ultra-fine grained materials," Scripta materialia, vol. 35, no. 2, 1996. doi: 10.1016/1359-6462(96)00107-8.

[14] M. Soltantabar and A. J. v. Ali, "Finite element analysis of copper deformed by conventional forward extrusion," IOSR J. Mech. Civ. Eng, vol. 10, pp. 1-5, 2014. doi: 10.9790/1684-1060105.

[15] I. Mazurina, T. Sakai, H. Miura, O. Sitdikov, R. J. M. S. Kaibyshev, and E. A, "Grain refinement in aluminum alloy 2219 during ECAP at 250 C," Materials Science and Engineering: A, vol. 473, no. 1-2, pp. 297-305, 2008. doi: 10.1016/j.msea.2007.04.112.

[16] V. J. M. S. Segal and E. A, "Slip line solutions, deformation mode and loading history during equal channel angular extrusion," Materials Science and Engineering: A, vol. 345, no. 1-2, pp. 36-46, 2003. doi: 10.1016/S0921-5093(02)00258-7.

[17] S.-B. Xu, Q. Zhen, L. Ting, C.-N. Jing, and G.-C. J. T. o. N. M. S. o. C. Ren, "Effect of severe plastic deformation on microstructure and mechanical properties of bulk AZ31 magnesium alloy," Transactions of Nonferrous Metals Society of China, vol. 22, pp. s61-s67, 2012.

[18] S. Wang, W. Liang, Y. Wang, L. Bian, and K. J. J. o. m. p. t. Chen, "A modified die for equal channel angular pressing," Journal of Materials Processing Technology, vol. 209, no. 7, pp. 3182-3186, 2009. doi: 10.1016/j.jmatprotec.2008.07.022.

[19] A. Panigrahi et al., "Effect of back pressure on material flow and texture in ECAP of aluminum," in IOP Conference Series: Materials Science and Engineering, 2014, vol. 63, no. 1, p. 012153: IOP Conference Series: Materials Science and Engineering. doi: 10.1088/1757-899X/63/1/012153.

[20] R. Y. J. J. o. m. s. Lapovok, "The role of back-pressure in equal channel angular extrusion," Journal of materials science, vol. 40, pp. 341-346, 2005. doi: 10.1007/s10853-005-6088-0.

[21] J. R. Bowen, A. Gholinia, S. Roberts, P. J. M. S. Prangnell, and E. A, "Analysis of the billet deformation behaviour in equal channel angular extrusion," Materials Science and Engineering: A, vol. 287, no. 1, pp. 87-99, 2000. doi: 10.1016/S0921-5093(00)00834-0.

[22] L. Kunčická and R. J. B. o. A. M. Kocich, "Influence of friction factor on deformation behaviour of the AA6063 alloy during ECAP; FE analysis," Bulletin of Applied Mechanics, vol. 9, no. 35, pp. 46-50, 2014.

[23] R. Parshikov, A. Rudskoy, A. Zolotov, and O. J. R. A. M. S. Tolochko, "Technological problems of equal channel angular pressing," Rev. Adv. Mater. Sci, vol. 34, pp. 26-36, 2013.

[24] A. Fardi Ilkhchy, M. J. A. J. o. M. Shaban Ghazani, and Simulation, "Finite element analysis of the Non-Equal Channel Angular Pressing (NECAP) with different die geometries," Journal of Advanced Materials and Processing, vol. 53, no. 2, pp. 81-92, 2021.

[25] S. Chung, H. Somekawa, T. Kinoshita, W. Kim, and K. J. S. M. Higashi, "The non-uniform behavior during ECAE process by 3-D FVM simulation," Scripta Materialia, vol. 50, no. 7, pp. 1079-1083, 2004. doi: 10.1016/j.scriptamat.2003.11.062.

[26] A. Gholinia, P. Prangnell, and M. J. A. M. Markushev, "The effect of strain path on the development of deformation structures in severely deformed aluminium alloys processed by ECAE," Acta Materialia, vol. 48, no. 5, pp. 1115-1130, 2000. doi: 10.1016/S1359-6454(99)00388-2.

[27] M. Furukawa, Z. Horita, M. Nemoto, and T. J. J. o. m. s. Langdon, "Processing of metals by equal-channel angular pressing," Journal of materials science, vol. 36, pp. 2835-2843, 2001. doi: 10.1023/A:1017932417043.

[28] M. Roshan, S. J. Jahromi, R. J. J. o. A. Ebrahimi, and Compounds, "Predicting the critical pre-aging time in ECAP processing of age-hardenable aluminum alloys," Journal of Alloys and Compounds, vol. 509, no. 30, pp. 7833-7839, 2011. doi: 10.1016/j.jallcom.2011.05.025.

[29] C. Cepeda-Jiménez, J. García-Infanta, O. A. Ruano, F. J. J. o. A. Carreño, and Compounds, "High strain rate superplasticity at intermediate temperatures of the Al 7075 alloy severely processed by equal channel angular pressing," Journal of Alloys and Compounds, vol. 509, no. 40, pp. 9589-9597, 2011. doi: 10.1016/j.jallcom.2011.07.076.

[30] M. S. El-Asfoury, M. N. Nasr, and A. J. T. o. t. I. I. o. M. Abdel-Moneim, "Non-equal Channel Multi-Angular Extrusion (NECMAE): A Design for Severe Plastic Deformation—Proof of Concept," Transactions of the Indian Institute of Metals, vol. 72, pp. 2827-2838, 2019. doi: 10.1007/s12666-019-01759-0

[31] M. S. El-Asfoury, M. N. Nasr, and A. Abdel-Moneim, "Effect of Friction on Material Mechanical Behaviour in Non-equal Channel Multi Angular Extrusion (NECMAE)," in Book of Abstracts, 2015, p. 364. doi: 10.2495/HPSM160101.

[32] M. J. E. m. s. Ohring, "How engineering materials are strengthened and toughened," vol. 1, ed. Engineering materials science: Academic Press San Diego, CA, USA, 1995, pp. 431-500.

[33] I. Balasundar, M. S. Rao, T. J. M. Raghu, and Design, "Equal channel angular pressing die to extrude a variety of materials," Materials & Design, vol. 30, no. 4, pp. 1050-1059, 2009. doi: 10.1016/j.matdes.2008.06.057.

[34] Y.-L. Yang and S. J. J. o. M. P. T. Lee, "Finite element analysis of strain conditions after equal channel angular extrusion," Journal of Materials Processing Technology, vol. 140, no. 1-3, pp. 583-587, 2003. doi: 10.1016/S0924-0136(03)00796-9.

[35] T. Suo, Y. Li, Q. Deng, Y. J. M. S. Liu, and E. A, "Optimal pressing route for continued equal channel angular pressing by finite element analysis," Materials Science and Engineering: A, vol. 466, no. 1-2, pp. 166-171, 2007. doi: 10.1016/j.msea.2007.02.068.

[36] N. Krywopusk, L. Kecskes, and T. J. M. C. Weihs, "The effect of strain rate on the microstructural evolution of pure Mg during ECAE," Materials Characterization, vol. 178, p. 111209, 2021. doi: 10.1016/j.matchar.2021.111209.

[37] M. Esmailzadeh and M. J. C. M. S. Aghaie-Khafri, "Finite element and artificial neural network analysis of ECAP," Computational Materials Science, vol. 63, pp. 127-133, 2012. doi: 10.1016/j.commatsci.2012.05.075.

[38] S.-y. J. T. o. N. M. S. o. C. Li, "Application of crystal plasticity modeling in equal channel angular extrusion," Transactions of Nonferrous Metals Society of China, vol. 23, no. 1, pp. 170-179, 2013. doi: 10.1016/S1003-6326(13)62444-9.

[39] J. Wongsa-Ngam, N. Noraphaiphipaksa, C. Kanchanomai, and T. G. J. C. Langdon, "Numerical Investigation of Plastic Strain Homogeneity during Equal-Channel Angular Pressing of a Cu-Zr Alloy," Crystals, vol. 11, no. 12, p. 1505, 2021. doi: 10.3390/cryst11121505.

[40] V. J. M. Segal, "Equal-channel angular extrusion (ECAE): from a laboratory curiosity to an industrial technology," Metals, vol. 10, no. 2, p. 244, 2020. doi: 10.3390/met10020244.

[41] Y. Estrin and A. J. A. m. Vinogradov, "Extreme grain refinement by severe plastic deformation: A wealth of challenging science," Acta materialia, vol. 61, no. 3, pp. 782-817, 2013. doi: 10.1016/j.actamat.2012.10.038.

[42] H. Khanlari and M. J. T. o. t. I. I. o. M. Honarpisheh, "Investigation of microstructure, mechanical properties and residual stress in non-equal-channel angular pressing of 6061 aluminum alloy," Transactions of the Indian Institute of Metals, vol. 73, pp. 1109-1121, 2020. doi.org/10.1007/s12666-020-01945-5.

[43] M. Asgari, F. Fereshteh-Saniee, S. M. Pezeshki, M. J. M. S. Barati, and E. A, "Non-equal channel angular pressing (NECAP) of AZ80 Magnesium alloy: Effects of process parameters on strain homogeneity, grain refinement and mechanical properties," vol. 678, pp. 320-328, 2016. doi.org/10.1016/j.msea.2016.09.102.